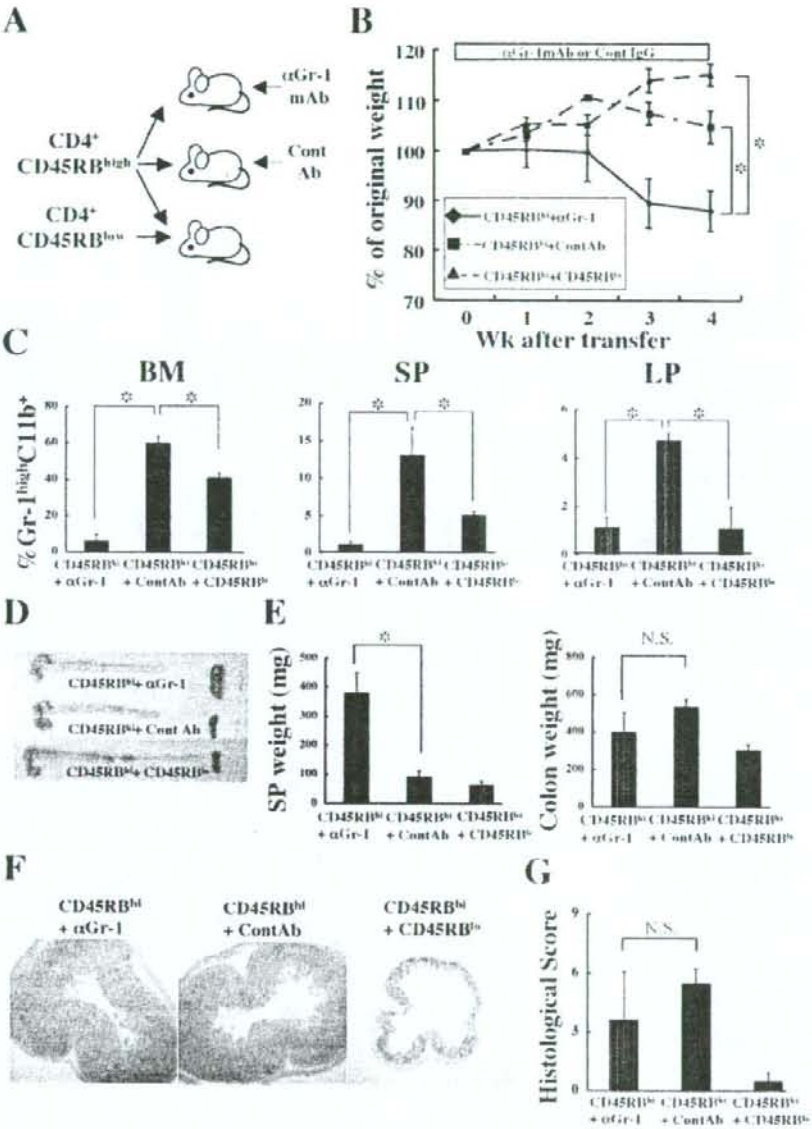

FIGURE 7. Anti-Gr-1 mAb treatment does not ameliorate colitis, but exacerbated wasting disease. A: Recipient SCID mice were administered anti-Gr-1 mAb or control rat IgG for 4 weeks starting from the time of $CD4^+CD45RB^{high}$ T-cell transfer. Other SCID control mice were transferred with $CD4^+CD45RB^{high}$ T cells and $CD4^+CD45RB^{low}$ T cells. All mice were sacrificed at 4 weeks after transfer. B: Change in body weight over time is expressed as percent of the original weight. Data are represented as mean ± SEM of 7 mice in each group. $^*P < 0.05$. C: Mice were analyzed by FACS for the expression of Gr-1 and CD11b cell-surface markers. D: Proportion of $Gr\text{-}1^{high}CD11b^+$ cells in BM, SP, and LP. Data are represented as mean ± SEM of 7 mice in each group. E: Gross appearance of the colon, spleen, and mesenteric lymph nodes. F: Weight of the colon and spleen. Data are represented as mean ± SEM of 7 mice in each group. $^*P < 0.05$. NS, not significantly different. G: Histological examination of the colon. Original magnification, ×100. H: Histological scoring. Data are indicated as the mean ± SEM of 7 mice in each group. NS, not significantly different.

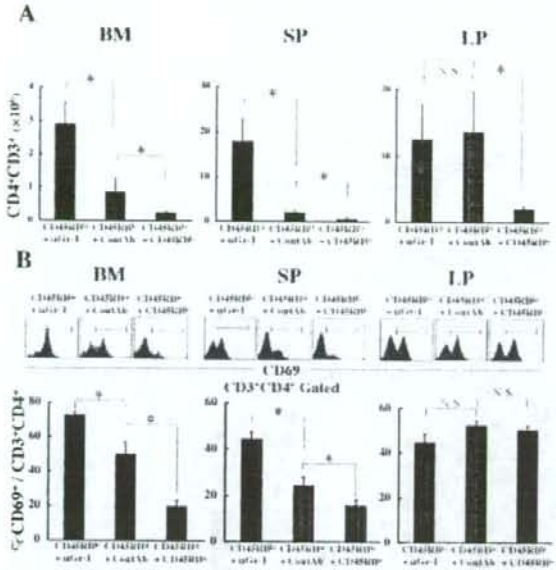

FIGURE 8. Anti-Gr-1 mAb treatment induces marked expansion of CD4$^+$ T cells in bone marrow and spleen of colitic mice. A: BM, SP, and LP CD4$^+$ T cells were isolated from SCID mice 4 weeks after transfer of CD4$^+$CD45RB^{high} cells and administration with anti-Gr-1 mAb or control rat IgG, or transfer of CD4$^+$CD45RB^{high} and CD4$^+$CD45RB^{low} cells. The absolute number of CD3$^+$CD4$^+$ cells was determined by flow cytometry. Data are indicated as mean ± SEM of 7 mice in each group. *$P < 0.05$. NS, not significantly different. B: The ratio of CD69$^+$ activated cells per total CD4$^+$ cells in BM, SP, and LP. Data are indicated as mean ± SEM of 7 mice in each group. *$P < 0.05$. NS, not significantly different.

We again confirmed that administration of anti-Gr-1 mAb preferentially depleted Gr-1^{high}CD11b$^+$ granulocytes, but not Gr-1^{low}CD11b$^+$ monocytes in SP (Fig. 7C). Consistent with the above-mentioned results (Figs. 1, 2), the proportion of Gr-1^{high}CD11b$^+$ granulocytes at 4 weeks after transfer was significantly increased in the BM, SP, and LP in the control IgG-treated mice as compared with the mice transferred with CD4$^+$CD45RB^{high} and CD4$^+$CD45RB^{low} cells (Fig. 7D). Furthermore, the depletion of granulocytes in the anti-Gr-1 mAb-treated mice was confirmed by the marked decrease of Gr-1^{high}CD11b$^+$ cells in these mice (Fig. 7C,D). At 4 weeks after transfer the colon from the control IgG- or anti-Gr-1-treated mice transferred with CD4$^+$CD45RB^{high} cells, but not that from mice transferred with CD4$^+$CD45RB^{high} and CD4$^+$CD45RB^{low} cells, was shortened and enlarged with a greatly thickened wall (Fig. 7E). Of note, the spleen of anti-Gr-1-treated mice was markedly enlarged as compared with that of the control IgG-treated mice and the mice transferred with CD4$^+$CD45RB^{high} and CD4$^+$CD45RB^{low} cells. This difference statistically confirmed that the weight of the spleen (Fig. 7F, left), but not the colon (Fig. 7F, right), of the anti-Gr-1-treated mice was significantly increased as compared with that of the control IgG-treated mice.

Histological examination showed prominent epithelial hyperplasia and glandular elongation with a massive infiltration of mononuclear cells in LP of the colon from the control IgG- or anti-Gr-1-treated mice (Fig. 7G). In contrast, the inflammation was mostly abrogated and only a few mononuclear cells were observed in LP of the colon from the mice transferred with CD4$^+$CD45RB^{high} and CD4$^+$CD45RB^{low} cells (Fig. 7G). This difference was also confirmed by histological scoring of multiple colon sections, which was 5.5 ± 0.71 in the control IgG-treated mice, 3.6 ± 2.46 in the anti-Gr-1-treated mice, and 0.5 ± 0.41 in the mice transferred with CD4$^+$CD45RB^{high} and CD4$^+$CD45RB^{low} T cells (Fig. 7H). Of note, the difference of histological score between the control IgG-treated mice and the anti-Gr-1-treated mice was not significant (Fig. 7H).

In Vivo Depletion of Granulocytes Induces Marked Expansion of CD4$^+$ T Cells with Activated Phenotype

A further quantitative evaluation of CD4$^+$ T-cell expansion was made by isolating mononuclear cells from various sites. The recovered cell number of LP CD4$^+$ T cells was significantly increased in the control IgG- or anti-Gr-1-treated mice as compared with that in the mice transferred with CD4$^+$CD45RB^{high} and CD4$^+$CD45RB^{low} cells, but the differences between the control IgG- and anti-Gr-1-treated mice was not significant (Fig. 8A, right). In contrast to the colonic infiltration of CD4$^+$ cells, the numbers of SP and BM CD4$^+$ T cells from the anti-Gr-1-treated mice were markedly increased as compared with those from the control IgG-treated mice (Fig. 8A, left and middle). Furthermore, the ratio of CD69$^+$ cells in total CD4$^+$ cells in the SP and BM, but not in the LP, from the anti-Gr-1-treated mice was significantly increased as compared with that from the control-IgG-treated mice (Fig. 8B), indicating that the granulocyte depletion induced a marked expansion of CD4$^+$ cells with activated phenotype.

Increased Granulopoiesis Is Induced in Splenectomized CD4$^+$CD45RB^{high} T-cell-transferred SCID Mice

Although we so far focused on the BM for the increased granulopoiesis in colitic mice, it remained possible that the marked increase of granulocytes in various sites of CD4$^+$CD45RB^{high} T-cell-transferred SCID mice was mainly due to extramedullary granulopoiesis in the spleen that is a representative site for it, but not in the BM. To evaluate this possibility we finally prepared age-matched SCID mice with or without splenectomy (SPX). Two weeks after recovery

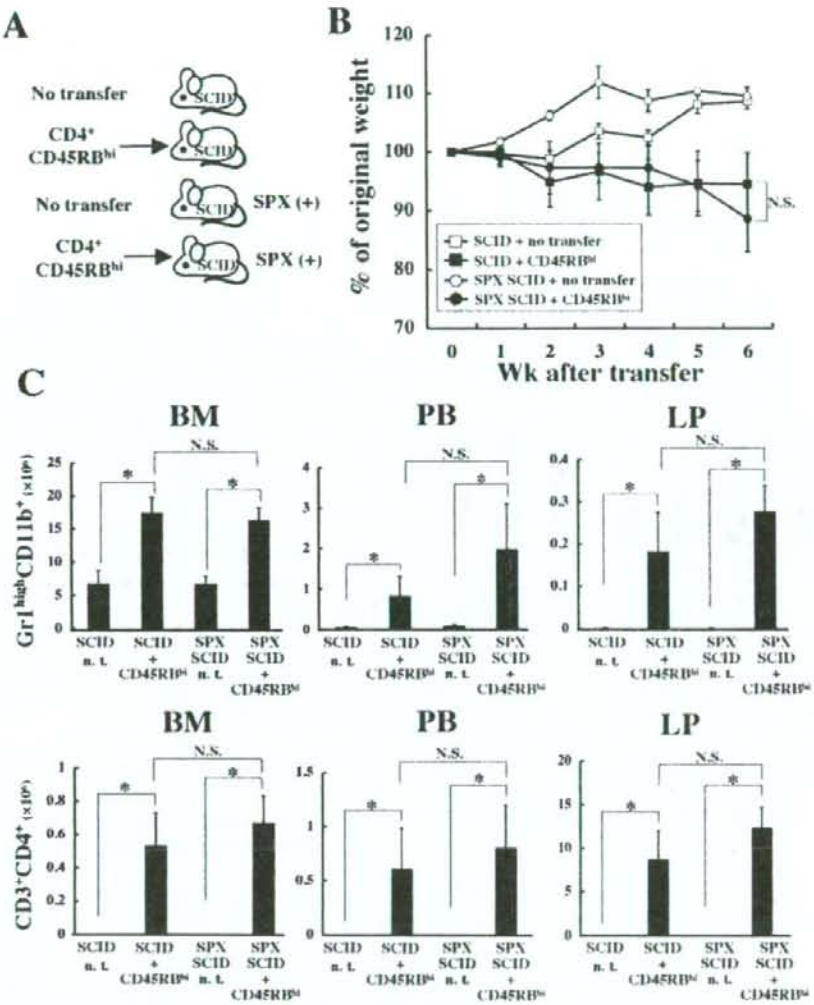

FIGURE 9. Splenectomized SCID mice transferred with CD4$^+$CD45RB^{high} T cells develop marked granulopoiesis. A: SCID mice were splenectomized 2 weeks before CD4$^+$CD45RB^{high} T-cell transfer. Mice were divided into 4 groups (each, $n = 5$) as follows; Group 1, SCID mice without splenectomy and without the transfer of CD4$^+$CD45RB^{high} T cells; Group 2, SCID mice without splenectomy and with the transfer of CD4$^+$CD45RB^{high} T cells; Group 3, SCID mice with splenectomy and without the transfer of CD4$^+$CD45RB^{high} T cells; and Group 4, SCID mice with splenectomy and with the transfer of CD4$^+$CD45RB^{high} T cells. All mice were sacrificed at 6 weeks posttransfer. SPX, splenectomy. B: Change in body weight over time is expressed as percent of the original weight. Data are represented as the mean ± SEM of 7 mice in each group. *$P < 0.05$. C: Absolute number of Gr-1^{high}CD11b$^+$ granulocytes or CD3$^+$CD4$^+$ T cells in the BM, PB, and LP. Data are represented as mean ± SEM of 7 mice in each group. nt, no transfer.

from surgery the SCID mice with or without SPX were transferred with CD4$^+$CD45RB^{high} T cells and were monitored for 6 weeks posttransfer (Fig. 9A). We found that SCID mice transferred with CD4$^+$CD45RB^{high} T cells irrespective of SPX developed a wasting disease (Fig. 9B) and clinical signs of colitis (data not shown). Also of note, the number of CD11b$^+$Gr-1^{high} granulocytes (Fig. 9C, upper) or CD3$^+$CD4$^+$ T cells (Fig. 9C, lower) was significantly increased in BM, PB, and LP to a similar extent irrespective of SPX, as compared with the paired SCID mice with no transfer, suggesting little contribution of spleen for the increased number of granulopoiesis in this colitis model.

Delayed Administration of Anti-Gr-1 mAb Induces Marked Expansion of Systemic CD4$^+$ T Cells

We next evaluated the effect of delayed administration of anti-Gr-1 mAb on the expansion of systemic CD4$^+$ T cells to assess the role of granulocytes in the process of ongoing disease (Fig. 10A). Since a wasting disease started 3 weeks after transfer (Fig. 10B), and the infiltration of lymphocytes and colitis was already detectable at 2 weeks (data not shown), we started the anti-Gr-1 mAb treatment from 3 weeks after transfer. As shown in Figure 10B, the anti-Gr-1 mAb-treated mice exhibited a significant exacerbation of weight loss as compared with the control IgG-treated mice. In contrast, control mice transferred with both CD4$^+$CD45RB^{high} and CD4$^+$CD45RB^{low} T cells did not exhibit a wasting disease (Fig. 10B). Furthermore, the proportion of Gr-1^{high}CD11b$^+$ granulocytes at 6 weeks after transfer was significantly increased in the SP and LP in the control IgG-treated mice as compared with the mice transferred with CD4$^+$CD45RB^{high} and CD4$^+$CD45RB^{low} cells (Fig. 10C), and the depletion of granulocytes by the anti-Gr-1 mAb treatment induced the marked decrease of Gr-1^{high}CD11b$^+$ cells in those mice (Fig. 10C). Nevertheless, the spleen of anti-Gr-1-treated mice was markedly enlarged as compared with that of the control IgG-treated mice and the mice transferred with CD4$^+$CD45RB^{high} and CD4$^+$CD45RB^{low} T cells (data not shown). Furthermore, histological assessment revealed that both mice treated with control IgG or anti-Gr-1 mAb developed severe colitis to a similar extent (Fig. 10D), with no statistical difference (data not shown). As seen in the protocol treated antibodies from 0 weeks after transfer (Figs. 8, 9), the number of CD3$^+$CD4$^+$ T cells in SP, but not in LP, from anti-Gr-1-treated mice was significantly increased as compared with control IgG-treated mice in spite of the delayed administration protocol (Fig. 10E).

DISCUSSION

In this study we demonstrated that the increased granulopoiesis in colitic BM plays a negative regulatory role to suppress the expansion of colitogenic T cells and wasting disease in a murine model of chronic colitis induced by adoptive transfer of CD4$^+$CD45RB^{high} T cells into SCID mice. We found that Gr-1^{high}CD11b$^+$ granulocytes in colitic PB were significantly increased even after the establishment of chronic colitis, and the depletion of granulocytes allowed the expansion of colitogenic CD4$^+$ T cells with activated phenotype, resulting in severe wasting disease.

Most studies have so far focused on the capacity of innate immune cells to shape adaptive immunity, and thus relatively little attention has been paid to the potential influence of acquired immunity on the innate immune system. For example, in the pathogenesis of chronic colitis it is thought that the early emerging immune cells in inflamed mucosa at the initial attack and at the recurrence of the diseases are granulocytes and macrophages before the activation of antigen-specific CD4$^+$ T cells.[1,2] These innate immune cells are thought to function as a first defense in injured mucosal tissues, and produce chemokines and proinflammatory cytokines to recruit acquired-immune CD4$^+$ T cells.[9] At the chronic phase of colitis after the establishment of colitogenic effector CD4$^+$ T cells, however, the role of granulocytes is almost ignored. Clinicopathologically, however, it has been established as a clinical score system that the degree of granulocyte infiltration in inflamed mucosa is a criteria for disease severity in both Crohn's disease[22] and ulcerative colitis.[23] According to these score systems, the degree of granulocyte infiltration correlates with pathological severity. Furthermore, it has also been reported that the circulating activated granulocytes are elevated with increased survival time in patients with severe IBD.[14,15] However, it still remains unclear whether the local and systemic activation of the granulocytes in severe IBD is pathogenic or protective.

In this regard, we adopted a direct approach using granulocyte-depleting anti-Gr-1 mAb in an in vivo study, and found that the administration of granulocyte-depleting anti-Gr-1 mAb did not affect the development of chronic colitis by assessing the histological scores and the expansion of LP CD4$^+$ T cells, but surprisingly induced a marked expansion of CD4$^+$ T cells with activated phenotype (CD69$^+$) in the SP and BM, resulting in a severer wasting disease as compared with the control IgG-treated mice. Interestingly, we observed that the anti-Gr-1-treated mice revealed splenomegaly in spite of almost complete depletion of Gr-1$^+$ granulocytes in SP, and surprisingly a marked increased compartment in SP was CD4$^+$ T cell. In addition, we observed that the delayed administration of anti-Gr-1 mAb starting at 3 weeks after CD4$^+$CD45RB^{high} T cell transfer also induced the systemic expansion of CD4$^+$ T cells as compared with the recipient with no treatment. These results suggest that the expansion of pathogenic T cells is negatively regulated by the presence of granulocytes in the BM and SP of chronic colitic mice. In a very recent publication, however, Kühl et al[24] demonstrated that RAG-1$^{-/-}$ mice transferred with CD4$^+$CD45RB^{high} T cells and treated with anti-Gr-1 mAb had a more increased mortality than the control IgG-treated RAG-1$^{-/-}$ mice transferred with CD4$^+$CD45RB^{high} T cells, but the difference of histological score between the 2 groups was not significant. Although they did not assess the systemic immune system in their study, they concluded that the discrepancy was due to the higher mortality and that the colitis in anti-Gr-1-treated mice was so severe that all mice eventually died from colitis. However, it remains possible that the marked increase of the systemic expansion of colitogenic CD4$^+$ T cells that produce a large amount of cachexia-inducing cytokines including TNF-α[17] as demonstrated in our present study induced a severe wasting disease rather than severe local inflammation.

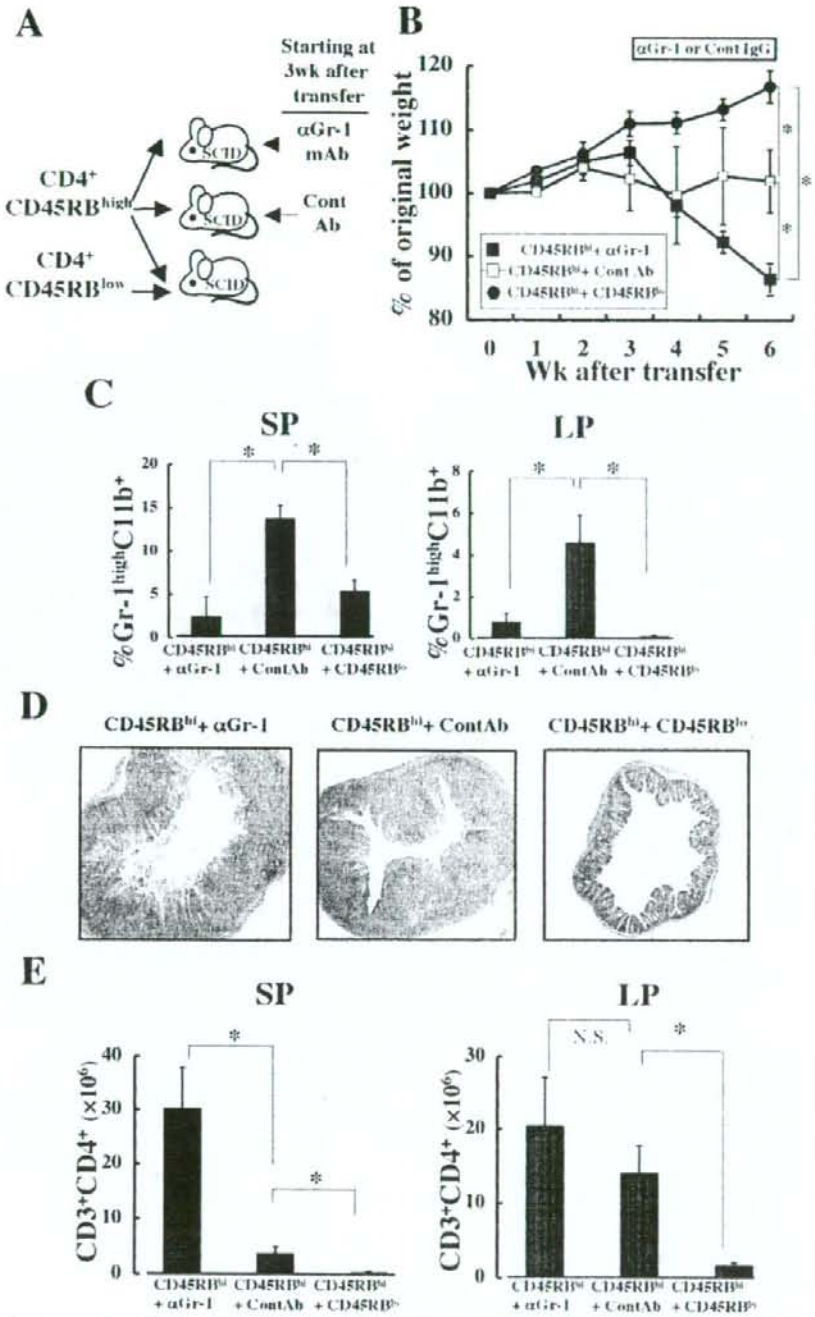

FIGURE 10. Delayed anti-Gr-1 mAb treatment does not ameliorate colitis, but increased systemic $CD4^+$ T cells. A: Recipient SCID mice were administered anti-Gr-1 mAb or control rat IgG for 3 weeks starting from 3 weeks after transfer. Other SCID control mice were transferred with $CD4^+CD45RB^{high}$ T cells and $CD4^+CD45RB^{low}$ T cells. All mice were sacrificed at 6 weeks after transfer. B: Change in body weight over time is expressed as percent of the original weight. Data are represented as mean ± SEM of 7 mice in each group. $^*P < 0.05$. C: Proportion of $Gr\text{-}1^{high}CD11b^+$ cells in SP and LP. Data are represented as mean ± SEM of 7 mice in each group. D: Histological examination of the colon. Original magnification, ×100. E: SP and LP $CD4^+$ T cells were isolated from SCID mice 6 weeks after transfer. The absolute number of $CD3^+CD4^+$ cells was determined by flow cytometry. Data are indicated as mean ± SEM of 7 mice in each group. $^*P < 0.05$. NS, not significantly different.

1501

Consistent with this, we here showed that the main increased sites of granulocytes were PB, SP, and BM rather than LP in colitic mice (Fig. 2). Further study will be needed to conclude this issue.

Although granulocytes make an important contribution to the recruitment of antigen-presenting cells, resulting in the T-cell activation and expansion at least in the initial phase of inflammation,[1,2] it has been proposed that Gr-1$^+$CD11b$^+$ cells induced in various pathological conditions including tumor, traumatic stress, bacterial, and parasitic infections, designated myeloid-derived suppressor cells or myeloid suppressor cells, have an ability to suppress T-cell activation.[25–27] For example, it has been demonstrated that activated granulocytes can impair TCR ζ-chain expression and cytokine production by T cells in advanced cancer.[28] Although we demonstrated that Gr-1^{high}CD11b$^+$ cells in the present colitis model do not express CD31, it is conceivable that the increased granulocytes at the late phase of chronic colitis also function as a novel suppressor against colitogenic CD4$^+$ T cells by a negative feedback loop.

Furthermore, the notion that granulocytes suppress the expansion of colitogenic CD4$^+$ T cells in chronic colitis may be relevant to the recent clinical usage of G-CSF and GM-CSF for patients with IBD.[29,30] A recent randomized controlled trial of 124 patients with severe-moderate Crohn's disease revealed a significant benefit of GM-CSF administration in response and in remission.[31] Although the authors speculated that normalization of innate immune function by the administration is one of the reasons for its effectiveness, our current study may suggest a possibility that the secondarily increased granulocytes directly suppress the activation and expansion of colitogenic CD4$^+$ T cells as "a regulatory granulocytes" as found in this study.

We have recently demonstrated that colitogenic CD4$^+$ memory T cells reside in the BM in chronic colitic mice.[21] Although it was initially thought that this model of colitis is mediated by Th1-type immune responses,[32] it has recently been recognized that Th17-mediated immune responses are also involved in this model.[33] Furthermore, it is well known that IL-17 induces G-CSF production by BM stromal cells, and is recognized as a promoting factor for granulopoiesis.[34] We thus focused on granulopoiesis in the colitic BM in this model. Although it was possible that extramedullary granulopoiesis in SP is also involved in the systemic increase of granulocytes in colitic mice, we also clearly demonstrated that splenectomized SCID mice transferred with CD4$^+$CD45RB^{high} T cells also had a marked increase of granulocytes in BM to a similar extent of the non-splenectomized SCID recipients (Fig. 6), indicating a more specific contribution of BM for the granulopoiesis in colitic mice. Furthermore, our current results in colitic mice may coincide with a recent report by Monteiro et al[35] showing that resident CD4$^+$ T cells in BM support the granulopoiesis in the normal BM environment.

In conclusion, we have demonstrated that granulocytes may play a pivotal role in the suppression of expansion of systemic colitogenic CD4$^+$ T cells in the late phase of colitis by a feedback loop induced by colitogenic BM CD4$^+$ T cells themselves. This finding also may provide the therapeutic rationale of the G-CSF and GM-CSF therapies for IBD.

REFERENCES

1. Podolsky DK. Inflammatory bowel disease. *N Engl J Med.* 2002;347:417–429.
2. Baumgart DC, Carding SR. Inflammatory bowel disease: cause and immunobiology. *Lancet.* 2007;369:1627–1640.
3. Strober W, Fuss IJ, Blumberg RS. The immunology of mucosal models of inflammation. *Annu Rev Immunol.* 2002;20:495–549.
4. Elson CO, Cong Y, McCracken VJ, et al. Experimental models of inflammatory bowel disease reveal innate, adaptive, and regulatory mechanisms of host dialogue with the microbiota. *Immunol Rev.* 2005;206:260–276.
5. Sartor RB. Mechanisms of disease: pathogenesis of Crohn's disease and ulcerative colitis. *Nat Clin Pract Gastroenterol Hepatol.* 2006;3:390–407.
6. Xavier RJ, Podolsky DK. Unravelling the pathogenesis of inflammatory bowel disease. *Nature.* 2007;448:427–434.
7. Strober W, Fuss IJ, Mannon P. The fundamental basis of inflammatory bowel disease. *J Clin Invest.* 2007;117:514–521.
8. Bamias G, Cominelli F. Immunopathogenesis of inflammatory bowel disease: current concepts. *Curr Opin Gastroenterol.* 2007;23:365–369.
9. Nathan C. Neutrophils and immunity: challenges and opportunities. *Nat Rev Immunol.* 2006;6:173–182.
10. Medzhitov R, Janeway CA Jr. Decoding the patterns of self and nonself by the innate immune system. *Science.* 2002;296:298–300.
11. Nikolaus S, Bauditz J, Gionchetti P, et al. Increased secretion of pro-inflammatory cytokines by circulating polymorphonuclear neutrophils and regulation by interleukin 10 during intestinal inflammation. *Gut.* 1998;42:470–476.
12. Foell D, Kucharzik T, Kraft M, et al. Neutrophil derived human S100A12 (EN-RAGE) is strongly expressed during chronic active inflammatory bowel disease. *Gut.* 2003;52:847–853.
13. Sutherland LR, Xiao LF. 2004. Clinical trial design with an emphasis on indices to measure disease activity. In: Sartor RB, Sandborn WJ, eds. Inflammatory Bowel Diseases. 6th ed. Philadelphia: Elsevier; 2004:453–468.
14. Brannigan AE, O'Connell PR, Hurley H, et al. Neutrophil apoptosis is delayed in patients with inflammatory bowel disease. *Shock.* 2000;13:361–366.
15. McCarthy DA, Rampton DS, Liu YC. Peripheral blood neutrophils in inflammatory bowel disease: morphological evidence of in vivo activation in active disease. *Clin Exp Immunol.* 1991;86:489–493.
16. Powrie F, Leach MW, S. Mauze S, et al. Phenotypically distinct subsets of CD4$^+$ T cells induce or protect from chronic intestinal inflammation in C.B-17 scid mice. *Int Immunol.* 1993;5:1461–1471.
17. Totsuka T, Kanai T, Iiyama R, et al. Ameliorating effect of anti-inducible costimulator monoclonal antibody in a murine model of chronic colitis. *Gastroenterology.* 2003;124:410–421.
18. Uraushihara K, Kanai T, Ko K, et al. Regulation of murine inflammatory bowel disease by CD25$^+$ and CD25$^-$CD4$^+$ glucocorticoid-induced TNF receptor family-related gene$^+$ regulatory T cells. *J Immunol.* 2003;171:708–716.
19. Bronte V, Apolloni E, Cabrelle A, et al. Identification of a CD11b$^+$Gr-1$^+$CD31$^+$ myeloid progenitor capable of activating or suppressing CD8$^+$ T cells. *Blood.* 2000;96:3838–3846.
20. Makita S, Kanai T, Nemoto Y, et al. Intestinal lamina propria retaining CD4$^+$CD25$^+$ regulatory T cells is a suppressive site of intestinal inflammation. *J Immunol.* 2007;178:4937–4946.
21. Nemoto Y, Kanai T, Makita S, et al. Bone marrow retaining colitogenic

CD4+ T cells may be a pathogenic reservoir for chronic colitis. *Gastroenterology*. 2007;132:176–189.
22. D'Haens GR, Geboes K, Peeters M, et al. Early lesions of recurrent Crohn's disease caused by infusion of intestinal contents in excluded ileum. *Gastroenterology*. 1998;114:262–267.
23. Hanauer SB, Robinson M, Pruitt R, et al. Budesonide enema for the treatment of active, distal ulcerative colitis and proctitis: a dose-ranging study. U.S. Budesonide enema study group. *Gastroenterology*. 1998; 115:525–532.
24. Kühl AA, Kakirman H, Janotta M, et al. Aggravation of different types of experimental colitis by depletion or adhesion blockade of neutrophils. *Gastroenterology*. 2007;133:1882–1892.
25. Delano MJ, Scumpia PO, Weinstein JS, et al. MyD88-dependent expansion of an immature Gr-1^{+}CD11b^{+} population induces T cell suppression and Th2 polarization in sepsis. *J Exp Med*. 2007;204:1463–1474.
26. Rabinovich GA, Gabrilovich D, Sotomayor EM. Immunosuppressive strategies that are mediated by tumor cells. *Annu Rev Immunol*. 2007; 25:267–296.
27. Serafini P, Borrello I, Bronte V. Myeloid suppressor cells in cancer: recruitment, phenotype, properties, and mechanisms of immune suppression. *Semin Cancer Biol*. 2006;16:53–65.
28. Ezernitchi AV, Vaknin I, Cohen-Daniel L, et al. TCR zeta down-regulation under chronic inflammation is mediated by myeloid suppressor cells differentially distributed between various lymphatic organs. *J Immunol*. 2006;177:4763–4772.
29. Schmielau J, Finn OJ. Activated granulocytes and granulocyte-derived hydrogen peroxide are the underlying mechanism of suppression of T-cell function in advanced cancer patients. *Cancer Res*. 2001;61:4756–4760.
30. Korzenik JR, Podolsky DK. Evolving knowledge and therapy of inflammatory bowel disease. *Nat Rev Drug Discov*. 2006;5:197–209.
31. Korzenik JR, Dieckgraefe BK, Valentine JF, et al. Sargramostim for active Crohn's disease. *N Engl J Med*. 2005;352:2193–2201.
32. Powrie F, Leach MW, Mauze S, et al. Inhibition of Th1 responses prevents inflammatory bowel disease in scid mice reconstituted with CD45RB^{hi}CD4^{+} T cells. *Immunity*. 1994;1:553–562.
33. Yen D, Cheung J, Scheerens H, et al. IL-23 is essential for T cell-mediated colitis and promotes inflammation via IL-17 and IL-6. *J Clin Invest*. 2006;116:1310–1316.
34. Schwarzenberger P, Huang W, Ye P, et al. Requirement of endogenous stem cell factor and granulocyte-colony-stimulating factor for IL-17-mediated granulopoiesis. *J Immunol*. 2000;164:4783–4789.
35. Monteiro JP, Benjamin A, Costa ES, et al. Normal hematopoiesis is maintained by activated bone marrow CD4^{+} T cells. *Blood*. 2005;105: 1484–1491.

J Gastroenterol 2009; 44:173–182
DOI 10.1007/s00535-008-2284-4

Journal of Gastroenterology

Musashi-1 suppresses expression of Paneth cell-specific genes in human intestinal epithelial cells

Minekazu Murayama[1]*, Ryuichi Okamoto[1,2]*, Kiichiro Tsuchiya[1], Junko Akiyama[1]
Tetsuya Nakamura[1,2], Naoya Sakamoto[1], Takanori Kanai[1], and Mamoru Watanabe[1]

[1] Department of Gastroenterology and Hepatology, Graduate School, Tokyo Medical and Dental University, 1-5-45 Yushima, Bunkyo-ku, Tokyo 113-8519, Japan
[2] Department of Advanced Therapeutics in GI Diseases, Graduate School, Tokyo Medical and Dental University, Tokyo, Japan

Background. Musashi-1 (Msi-1) is a RNA-binding protein, known as a putative marker of intestinal stem cells (ISCs). However, little is known about the function of Msi-1 within human intestinal epithelial cells (IECs). Thus, the present study aimed to clarify the role of Msi-1 in differentiation and proliferation of IECs. ***Methods.*** A human intestinal epithelial cell line stably expressing Msi-1 was established. Proliferation of the established cell lines was measured by bromodeoxyuridine incorporation, whereas differentiation were assessed by reverse transcriptase-polymerase chain reaction (RT-PCR) analysis of lineage-specific genes. Activities of the Notch and Wnt pathways were examined either by reporter assays or expression of downstream target genes. The distribution of Msi-1 and PLA2G2A expression in vivo was determined by immunohistochemistry. ***Results.*** Constitutive expression of Msi-1 in IECs had no significant effect on cell proliferation, but suppressed expression of Paneth cell-specific genes, including *PLA2G2A*. Msi-1 appeared to suppress expression of the *PLA2G2A* gene at the mRNA level. Analysis of Notch and Wnt pathway activity, however, revealed no significant change upon Msi-1 expression. The expression of Msi-1 and PLA2G2A in vivo was restricted to IECs residing at the lowest part of the human intestinal crypt, but was clearly separated to within basal columnar cells or mature Paneth cells, respectively. ***Conclusions.*** Msi-1 suppresses expression of Paneth cell-specific genes in IECs, presumably through a pathway independent from Notch or Wnt. These findings suggest Msi-1 is a negative regulator of Paneth cell differentiation, an may contribute to maintain the undifferentiated phenotype of ISCs.

Received: July 22, 2008 / Accepted: August 16, 2008
Reprint requests to: K. Tsuchiya
* These authors contributed equally to this work.

Key words: Musashi-1, intestinal epithelial cells, Paneth cells, PLAG2A

Introduction

The rapid and continuous renewal of the intestinal epithelium is maintained by the regulated supply of newborn cells that arise from a common progenitor cell called the intestinal stem cell (ISC).[1] Such tissue-specific stem cells share common potentials to self renew and also to give rise to all cell lineages composing the residing tissue.[2] Such properties of stem cells are maintained by a complex interaction of various cell-signaling pathways.[3] Among such signaling pathways, Wnt and Notch represent the core molecular pathways that play crucial roles in maintaining stem cell properties.[4] Indeed, both Wnt and Notch signaling have been shown to function in intestinal crypt epithelial cells, including the ISCs.[5] A recent study identified Lgr-5, a direct target of the canonical Wnt pathway, as a definite marker of murine ISCs.[6] This study further emphasized the dominant role of the canonical Wnt pathway in maintaining cell proliferation and multipotency of ISCs. It is, however, known that activation of the canonical Wnt pathway is present not only in ISCs but also in Paneth cells residing just adjacent to ISCs, where it promotes maturation and restricts the cell position of such cells.[7] Thus, activation of the canonical Wnt pathway appears to have a completely different function in ISCs and Paneth cells, presumably depending on the cell context determined by other molecular factors. However, the molecular mechanism regulating such lineage-specific functions of canonical Wnt signaling in IECs remains largely unknown.

Musashi-1 (Msi-1) is an RNA-binding protein, and its gene was formerly reported as another candidate marker gene for ISCs.[8,9] Its molecular function has been deter-

mined as translational repression of target genes, such as *m-Numb*, a negative regulator of Notch signaling.[10] In both mice and humans, Msi-1 has been shown to be expressed in ISCs, but in sharp contrast, its expression is completely lacking in mature Paneth cells.[8,9,11] Thus, Msi-1 might function within intestinal epithelial cells (IECs) to maintain their undifferentiated state.[12,13] However, the molecular function of Msi-1 in IECs has never been described.

Herein, we show that expression of Msi-1 in IECs suppressed expression of Paneth cell-specific genes, such as *PLA2G2A*. Msi-1 appeared to downregulate expression of the *PLA2G2A* gene at the mRNA level, through a molecular pathway independent of both Notch and Wnt, the two major molecular pathways that are known to regulate Paneth cell differentiation. These results suggest that Msi-1 is a negative regulator of Paneth cell differentiation in IECs, and that it has a functional role in maintaining the undifferentiated state of ISCs.

Materials and methods

Cell culture

Human colon cancer-derived LS174T cells were cultured in minimal essential medium (GIBCO, Billings, MT, USA) supplemented with 10% fetal bovine serum, 2 mM L-glutamine, 100 U/ml penicillin, and 100 mg/ml streptomycin (Invitrogen, Carlsbad, CA, USA), at 37°C in a humidified incubator with 5% CO_2.

Plasmids

For construction of the expression plasmid for Msi-1 (pcDNA3.0-Msi-1), the entire coding lesion of the mouse *Msi-1* gene was polymerase chain reaction (PCR) amplified from pcDNA3.0-FLAG-Msi-1 (kindly provided by Dr. Hideyuki Okano), and inserted into pcDNA3.0 (Invitrogen). For construction of the enhanced green fluorescent protein (EGFP) expression plasmid (pCMV-FLAG-EGFP), the coding sequence of pEGFP-C1 (Stratagene, La Jolla, CA, USA) was PCR amplified and inserted into the pCMV-FLAG-Tag vector (Stratagene).

Establishment of cell lines stably expressing Msi-1 or EGFP

Expression plasmids for Msi-1 (pcDNA3.0-Msi-1) or EGFP (pCMV-FLAG-EGFP) were transfected into LS174T cells as previously described.[14] After 2 days of culture, cells were selected by addition of G418 (1 mg/ml) to the culture medium. Subsequently, G418-resistant cells were cloned into sublines expressing Msi-1 or EGFP, designated as LS174T/Msi-1 cells or LS174T/GFP cells, respectively.

Microscopic imaging and immunostaining of cultured cells

Microscopic images of cultured cells were collected using an epifluorescence microscope system (BZ-2000, Keyence, Osaka, Japan). Immunostaining of cultured cells were done as previously described.[15,16] For detection of Musashi-1, primary antibody (14H1, kindly provided by Dr. Hideyuki Okano) was diluted to 1:1000 and detected by an Alexa-488-conjugated secondary antibody (Molecular Probes, Eugene, OR USA). Cells were counterstained by 4′,6-diamino-2-phenylindole (DAPI), and mounted in Vectashield mounting medium (Vector Laboratories, Burlingame, CA, USA).

Cell proliferation assay

Incorporation of bromodeoxyuridine (Brd-U) was examined using a cell proliferation enzyme-linked immunosorbent assay (ELISA) kit (Roche Diagnostics, Mannheim, Germany), according to the manufacturer's instructions. Briefly, cells were seeded onto a 96-well dish at various cell densities, cultured for 48 h, and labeled with Brd-U for 8 h at the end of culture. Each condition was measured in triplicate and the results analyzed by Student's *t* test.

Reverse transcription-polymerase chain reaction

Total RNA was prepared using TRIzol reagent (Invitrogen) according to the manufacturer's instructions. Reverse transcription (RT) was carried out as previously described.[15] Forward and reverse primers used for the PCR reaction are summarized in Table 1. For semiquantitative PCR, 1 µl of cDNA was amplified with 0.25 U of LA *Taq* polymerase (Takara, Otsu, Japan), using the optimized amplification cycles determined for each primer set. Amplified products were separated by 1.8% agarose gel electrophoresis, stained with ethidium bromide, and visualized by the Lumi-Imager F1 system (Roche Diagnostics). For quantitative PCR, 1 µl of cDNA was amplified using SYBR green master mix (Qiagen, Valencia, CA, USA), and analyzed by a 7500 real-time PCR system (Applied Biosystems, Foster City, CA, USA).

Immunoblotting

Immunoblot analysis was done as previously described.[15] Briefly, 1×10^6 cells were seeded onto 6-cm culture dishes and collected for protein extraction after 48 h of

Table 1. Primers used in the present study

Gene	Primer sequence	
	Forward	Reverse
Musashi-1	5′-GGCTTCGTCACTTTCATGGACCAGGCG-3′	5′-GGGAACTGGTAGGTGTAAC-3′
MUC2	5′-CTGCACCAAGACCGTCCTCATG-3′	5′-GCAAGGACTGAACAAAGACTCAGAC-3′
TFF3	5′-TGAGGAGTACGTGGGCCTGTCTGCAAA-3′	5′-CGGGTGGAGCATGGGACCTTTATT-3′
KLF-4	5′-GGGAGAAGACACTGCGTCA-3′	5′-GGAAGCACTGGGGGAAGT-3′
Isomaltase	5′-TACTAGAAGACAAGATCCCGCT-3′	5′-GTAGTTCCTTTCCCCCATACAT-3′
Lactase	5′-CCCCAAAGCATCAGCGAAGTT-3′	5′- CTACACGTTTCCGCAAGAGCT-3′
PLA2G2A	5′-ACCATGAAGACCCTCCTACTG-3′	5′-GAAGAGGGGACTCAGCAACG-3′
HD-5	5′-CCCAGCCATGAGGACCATCG-3′	5′-TCTATCTAGGAAGCTCAGCG-3′
HD-6	5′-CCACTCCAAGCTGAGGATGATC-3′	5′-CCACTCCAAGCTGAGGATGATC-3′
Lysozyme	5′-CTCTCATTGTTCTGGGGC-3′	5′-ACGGACAACCCTCTTTGC-3′
c-Myc	5′-CTTCTGCTGGAGGCCACAGCAAACCTCCTC-3′	5′-CCAACTCCGGGATCTGGTCACGCAGGG-3′
EphB3	5′-AGCAACCTGGTCTGCAAAGT-3′	5′-TCCATAGCTCATGACCTCCC-3′
G3PDH	5′-TGAAGGTCGGAGTCAACGGATTTGGT-3′	5′-CATGTGGGCCATGAGGTCCACCAC-3′
GFP	5′-TGAAGGTCGGAGTCAACGGATTTGGT-3′	5′-CATGTGGGCCATGAGGTCCACCAC-3′

culture. Total cell lysate was prepared using radioimmunoprecipitation assay buffer. Fifty micrograms of each lysate was subjected to analysis. Primary antibodies used were as follows: mouse anti-Musashi-1 (1:500, Chemicon, Temecula, CA, USA), rabbit anti-GFP (1:2500, MBL, Nagoya, Japan), Goat anti-NUMB (1:100, Santa Cruz Biotechnology, Santa Cruz, CA, USA), rabbit anti-Hes1 (kindly provided by Dr. T. Sudo), mouse anti-β-actin (1:5000, Sigma, St. Louis, MO, USA). Primary antibodies were detected by the appropriate horseradish peroxidase-conjugated secondary antibodies, and visualized by the Lumi-Imager F1 system (Roche Diagnostics) using enhanced chemiluminescence (Amersham Biosciences, Buckinghamshire, UK) as a substrate.

Quantification of PLA2G2A secretion

For PLA2G2A protein quantification, 1×10^6 cells were seeded onto a 6-cm dish and cultured for up to 5 days. Supernatants were collected at 1, 3, and 5 days of culture and analyzed with a sPLA2 (human type IIA) enzyme immunoassay (EIA) kit (Cayman Chemical, Ann Arbor, MI, USA). The assay was performed in triplicate, and the results statistically analyzed by paired Student's *t* test.

Reporter assays

Reporter assays using the dual luciferase system (Promega, Madison, WI, USA) has been previously described.[15] TOP-Flash and FOP-Flash reporter plasmids were purchased from Upstate Biotechnology (Lake Placid, NY, USA). Each condition was examined in triplicate and the results analyzed by Student's *t* test.

Human intestinal tissue specimens

Normal human small intestinal tissues were obtained from patients who underwent surgery for the treatment of Crohn's disease at Yokohama Municipal General Hospital, and macroscopically intact regions of each specimen were subjected for immunohistochemical staining. Written informed consent was obtained from each patient, and the study was approved by the ethics committee of Yokohama Municipal General Hospital and Tokyo Medical and Dental University.

Immunohistochemistry

Immunohistochemistry using human intestinal tissues has been previously described.[11] Primary antibodies used were as follows: Rat anti-Musashi-1 (1:1000, kindly provided by Dr. Hideyuki Okano), and Goat-anti-human PLA2G2A (1:200, sc-14468, Santa Cruz Biotechnology). Microwave treatment (500 W, 10 min) in 10 mM citrate buffer was required for detection of both Msi-1 and PLA2G2A. Msi-1 antibody was visualized using Alexa-488-conjugated Tyramide (Molecular Probes) as a substrate for the avidin–biotin complex (Vector Laboratories), whereas PLA2G2A antibody was visualized by Alexa-594-conjugated secondary antibody (Molecular Probes). Sections were counterstained with DAPI and mounted in Vectashield mounting medium (Vector Laboratories). Fluorescent images were captured by the epifluorescence microscope system (BZ-2000, Keyence).

Results

Establishment of stable cell lines constitutively expressing Msi-1

To analyze the functional role of Msi-1, we planned to assess the effect of Msi-1 expression in human IECs. For this purpose, we employed LS174T cells as the parental (host) cells, as we have previously shown that these cells readily express a wide variety of lineage-specific genes,[15,16] but do not express detectable amount of endogenous Msi-1 protein (Fig. 1B). These features of LS174T cells makes them an ideal model for examining whether expression of Msi-1 can modulate proliferation as well as differentiation of human IECs. Following transfection of an expression plasmid for Msi-1, we successfully generated three clones of LS174T cells that stably expressed Msi-1 (designated hereafter as LS174T/Msi-1 cells). We also generated another clone of LS174T cells that stably expressed EGFP to serve as a control (LS174T/GFP cells). RT-PCR analysis of these generated cell clones revealed mRNA expression from the corresponding transgenes (Fig. 1A). Also, immunoblot analysis clearly showed expression of green fluorescent protein (GFP) or Msi-1 protein in LS174T/GFP or LS174T/Msi-1 cells, respectively (Fig. 1B). An epifluorescence view of these cells also assured constitutive expression of GFP in all of the LS174T/GFP cells but not in the other cell clones (Fig. 1C). In contrast, immunostaining of Msi-1 protein revealed constitutive expression of Msi-1 protein in all of the LS174T/Msi-1 cells but not in the other cell clones (Fig. 1D). A phase-contrast view showed no clear difference between parental cells and LS174T/GFP cells, as both cell clones aggregated to form a round cell colony consisting of vertically piled-up cells (Fig. 1C). LS174T/Msi-1 cells, however, failed to form such cell colonies, but showed a very flat cell morphology and appeared to spread horizontally as a monolayer of cells (Fig. 1C). These results collectively confirmed that the generated cells surely expressed GFP or Msi-1 protein in a constitutive manner, and also suggested that expression of Msi-1 might have induced some intracellular changes influencing the shape and nature of colony formation of LS174T cells.

Expression of Msi-1 did not change cell proliferation but decreased expression of Paneth cell-specific genes in LS174T cells

As we found morphological changes in cells and colony shape of LS174T/Msi-1 cells (Fig. 1C), we examined whether they underwent changes in cell proliferation. Analysis of Brd-U incorporation, however, showed no significant change in LS174T/Msi-1 cells compared with LS174T/GFP cells (Fig. 2A). Next, we analyzed the expression of lineage-specific genes, to evaluate the effect of Msi-1 expression upon IEC differentiation. Results of the RT-PCR analysis showed no change in expression of goblet cell-specific genes such as *MUC-2*, *TFF-3*, or *KLF-4* (Fig. 2B). Also, genes specific for absorptive cell lineage (Fig. 2B) or neuroendocrine cell lineage (data not shown) remained undetectable in both LS174T/GFP and LS174T/Msi-1 cells. In sharp contrast, expression of Paneth cell-specific genes such as *PLA2G2A*, *HD-5*, and *Lysozyme*[17] appeared to be decreased in LS174T/Msi-1 cells, compared with LS174T/GFP cells (Fig. 2B). This suggested that expression of Msi-1 might have suppressed expression of Paneth cell-specific genes in LS174T/Msi-1 cells.

To confirm our earlier results, we further examined the expression of one of the Paneth cell-specific genes, *PLA2G2A*, as it showed the clearest decrease in mRNA in LS174T/Msi-1 cells (Fig. 2B). Quantitative RT-PCR confirmed an up to 90% decrease of *PLA2G2A* mRNA expression in LS174T/Msi-1 cells, compared with LS174T/GFP cells (Fig. 3A). PLA2G2A protein secretion also showed a significant decrease in LS174T/Msi-1 cells compared with LS174T/GFP cells (Fig. 3B). From these results, Msi-1 appeared to suppress *PLA2G2A* gene expression at the mRNA level, leading to decreased secretion of mature PLA2G2A protein.

Expression of Msi-1 did not change the expression level of genes downstream of Notch and Wnt pathways in LS174T cells

As it is has been previously reported that one of the molecular functions of Msi-1 is translational repression of m-Numb, a negative regulator of Notch signaling,[10] we next examined whether suppression of *PLA2G2A* gene expression might be induced through modulation of the Notch signaling pathway. Immunoblot analysis of m-Numb or Hes1 expression, however, showed equivalent expression of both proteins in LS174T/Msi-1 and LS174T/GFP cells (Fig. 4A). Consistently, the reporter assay for RBP-Jk-dependent transcription showed no significant difference between LS174T/Msi-1 and LS174T/GFP cells (Fig. 4B). These results suggest that expression of Msi-1 had minimal effect upon expression of *m-Numb* or target genes of Notch in LS174T cells.

In addition to Notch, the Wnt signaling pathway has been described as another key signaling pathway for Paneth cell differentiation.[7,18] Also, *PLA2G2A* has been shown to be one of the direct target genes of the canonical Wnt pathway.[19] As a recent study reported that Msi-1 could modulate signaling of the Wnt pathway,[20] we next examined whether expression of Msi-1 had modulated the intracellular activity of the Wnt pathway. Consistent with the previous result in mammary

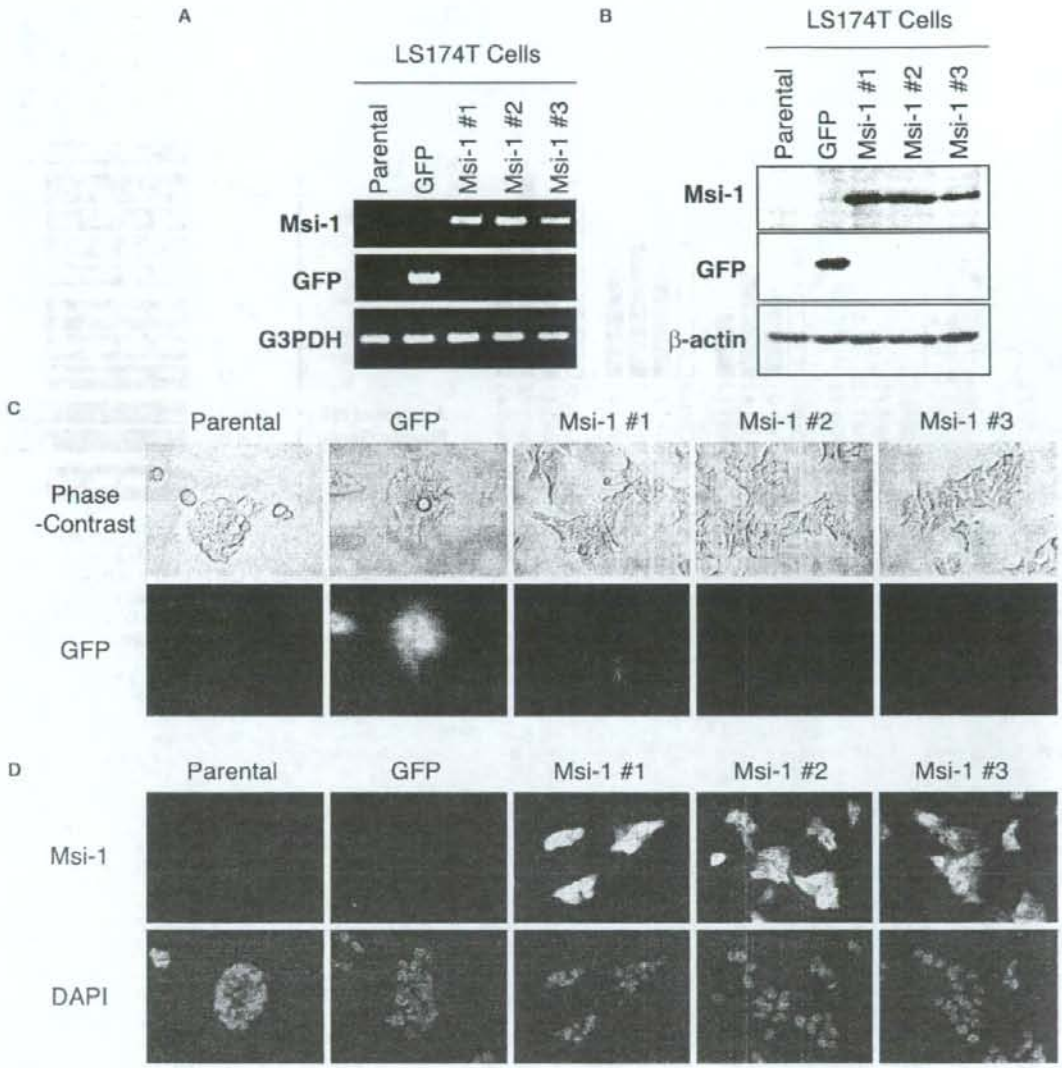

Fig. 1. Establishment of cell lines stably expressing Musashi-1. **A** Reverse transcriptase-polymerase chain reaction (RT-PCR) analysis of the generated cell lines. *GFP* (green fluorescent protein) indicates a clone of LS174T cells that constitutively expresses enhance green fluorescent protein (EGFP) (LS174T/GFP cells), whereas *Msi-1 #1*, *Msi-1 #2*, and *Msi-1 #3* indicate distinct clones of LS174T cell that constitutively express Musashi-1 (Msi-1) (LS174T/Msi-1 cells). *Parental* indicates the parental LS174T cells. Note that mRNA expression of Msi-1 or GFP is clearly observed in LS174T/GFP cells or LS174T/Msi-1 cells, respectively, but not in parental cells. **B** Immunoblot analysis of the generated cell lines. Total cell lysate obtained from each cell line was analyzed for expression of Msi-1, GFP, and β-actin. Msi-1 protein was detected exclusively in the LS174T/Msi-1 cell lines (Msi-1 #1, #2, and #3), whereas GFP protein was detected exclusively in LS174T/GFP cells (GFP). **C** Morphological changes and GFP expression in the generated cell lines. Phase contrast view of the cell lines shows aggregated, round colony formation in parental and LS174T/GFP cells (GFP), whereas a flat, monolayer expansion is observed in LS174T/Msi-1 cells (Msi-1 #1, #2, and #3). An epifluorescence view confirmed stable expression of GFP in LS174T/GFP cells, but not in other cells. **D** Expression of Msi-1 protein in generated cell lines. Cells were stained by Msi-1 specific antibody and visualized by Alexa-488-conjugated secondary antibody. Cells were also counterstained with 4′,6-diamino-2-phenylindole (DAPI). Staining confirmed the expression of Msi-1 protein in LS174T/Msi-1 cells (Msi-1 #1, #2, and #3), and not in other cells

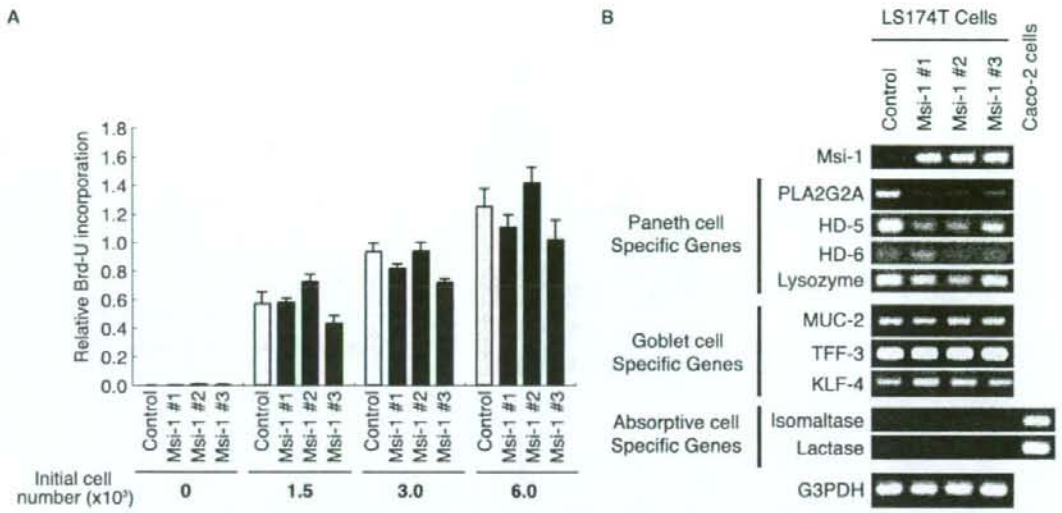

Fig. 2. Expression of Msi-1 does not change cell proliferation, but decreases expression of Paneth cell-specific genes in LS174T cells. **A** Bromodeoxyuridine (*Brd-U*) incorporation of the generated cell lines. Cells were cultured at various densities and subjected to Brd-U incorporation analysis using an enzyme-linked immunosorbent assay. Results of LS174T/GFP cells served as a control. Error bar represents SD. **B** Semiquantitative RT-PCR analysis of lineage-specific genes in the generated cell lines. Total RNA was isolated from LS174T/GFP cells (*Control*) or LS174T/Msi-1 cells (*Msi-1 #1*, *Msi-1 #2*, and *Msi-1 #3*), and subjected to analysis. A corresponding sample prepared from Caco-2 cells served as a positive control for absorptive cell-specific genes. Glyceraldehyde-3-phosphate dehydrogenase (*G3PDH*) served as an internal control

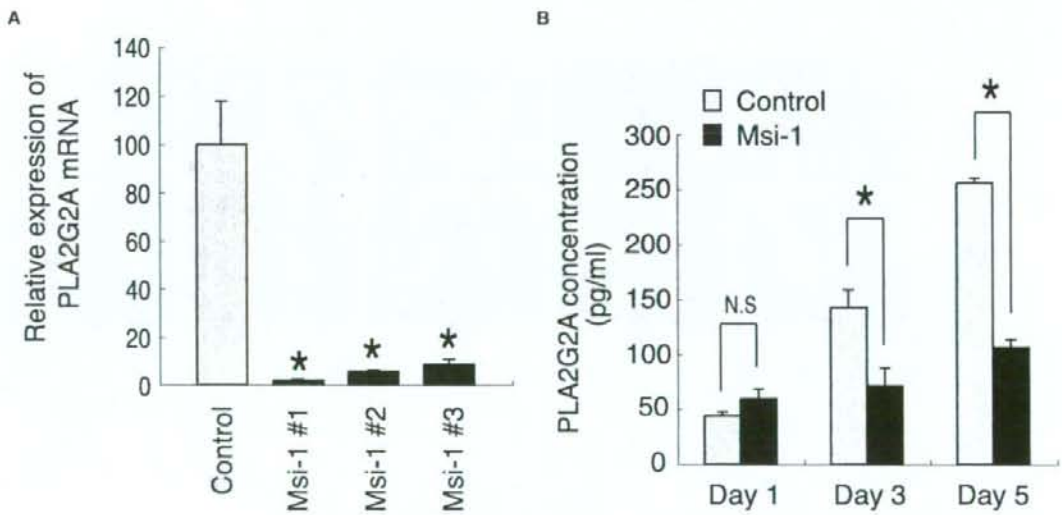

Fig. 3. Expression of Msi-1 suppresses gene expression of *PLA2G2A* in LS174T cells. **A** Quantitative RT-PCR analysis of *PLA2G2A* expression in the generated cell lines. Results of LS174T/GFP cells served as a control. Error bar represents SD. $^*P < 0.05$, Student's *t* test. **B** Analysis of PLA2G2A protein secretion by LS174T parental cells (*Control*) or LS174T/Msi-1 cells (*Msi-1*). Control or LS174T/Msi-1 cells were cultured for up to 5 days, and the amount of secreted PLA2G2A was measured by enzyme immunoassay at different time points. Error bar represents SD. $^*P < 0.05$, Student's *t* test

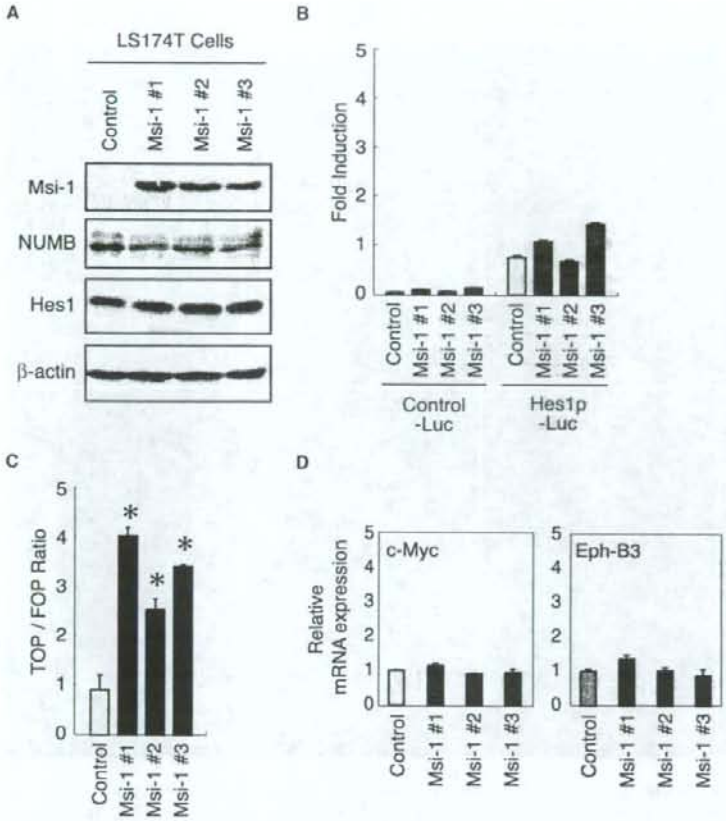

Fig. 4. Expression of Msi-1 has no effect upon expression of target genes downstream of Notch or Wnt pathways in LS174T cells. **A** Immunoblot analysis of Notch pathway genes in the generated cell lines. Total cell extract prepared from LS174T/GFP cells (*Control*) or LS174T/Msi-1 cells (*Msi-1 #1*, *Msi-1 #2*, and *Msi-1 #3*) was subjected to analysis. Result for *m-Numb* shows two distinct bands, one representing the short (*upper band*) and the other the long (*lower band*) isoform of the *m-Numb* gene. **B** Luciferase reporter assay for analysis of RBP-Jk dependent transcriptional activity. Hes1p-Luc contains six tandem repeats of RBP-Jk binding sites, whereas Control-Luc contains only the core promoter element derived from the chicken *β-actin* gene. Each data point was normalized by the corresponding Renilla luciferase activity. Error bar represents SD. **C** Luciferase reporter assay for analysis of TCF-dependent transcriptional activity. Firefly luciferase activity of the TOP-flash or FOP-flash vector was normalized by the corresponding Renilla luciferase activity. Data are shown as ratio of normalized TOP-flash and FOP-flash activity. Error bar represents SD. $*P < 0.05$ compared with control cells, Student's t test. **D** Quantitative RT-PCR analysis of Wnt target genes in the generated cell lines. Relative expression level of c-Myc and Eph-B3 are shown. Error bar represents SD. Expression in LS174T/GFP cells (*Control*) is set to 1

epithelial cells,[20] we found that TCF-dependent transcriptional activity was upregulated two- to four fold in LS174T/Msi-1 cells compared with LS174T/GFP cells (Fig. 4C). However, expression of c-Myc and Eph-B3 showed no significant change between LS174T/Msi-1 cells and LS174T/GFP cells (Fig. 4D), suggesting that an additional increase of TCF-dependent transcriptional activity in these cells may not necessarily lead to changes in the expression level of the downstream target genes. These results showed that expression of Msi-1 in LS174T cells has only a minimal effect upon Notch or Wnt target genes, and suggested that changes observed in LS174T/Msi-1 cells, such as cell morphology or *PLA2G2A* expression, are presumably mediated through a mechanism independent of such molecular signaling pathways.

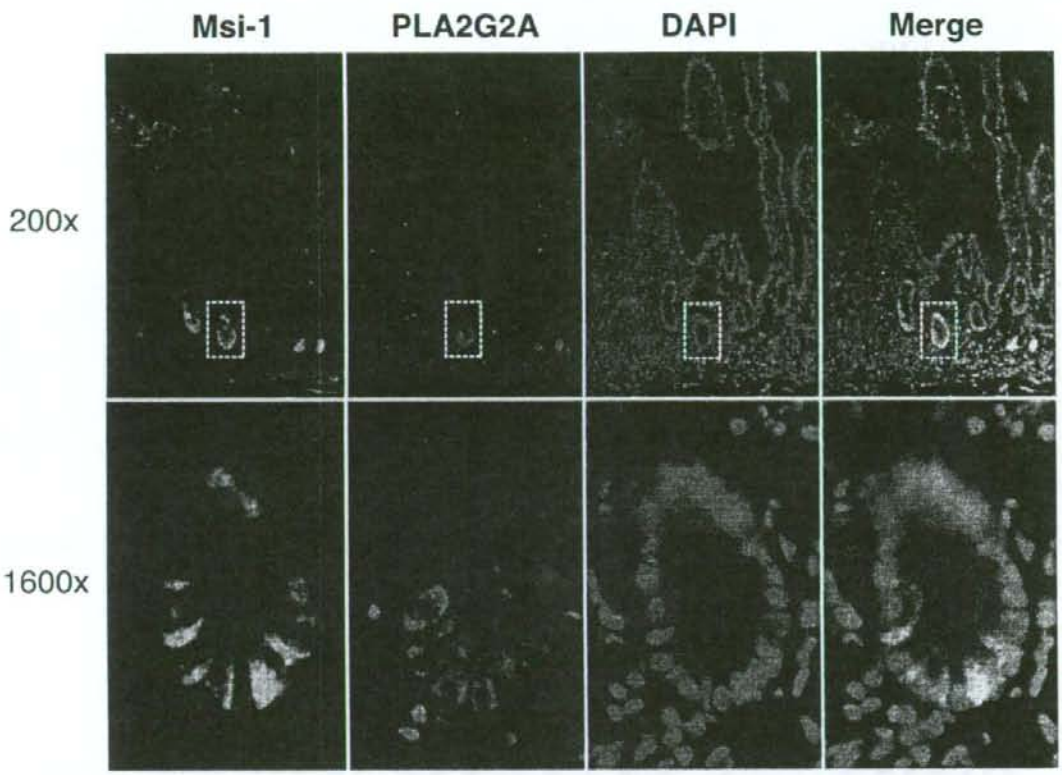

Fig. 5. Distinct cell population within the human intestinal crypt express Msi-1 or PLA2G2A. Double immunofluorescence staining of Msi-1 and PLA2G2A using a human small intestinal tissue is shown. Positive signals for both Msi-1 (*green*) and PLA2G2A (*red*) are observed in epithelial cells residing at the lowest part of the crypt (*upper panel*). A magnified view (*lower panel*) of the designated area (*white squares, upper panel*) shows positive staining of Msi-1 and PLA2G2A, each in distinct intestinal epithelial cells (IECs); coexpression of both proteins in a single IEC is not observed

Distinct populations of crypt epithelial cells expressed Msi-1 or PLA2G2A in the human intestine

To examine whether such a function of Msi-1 might be prevalent also in vivo, we examined the distribution of Msi-1- and PLA2G2A-expressing IEC's within the human intestine. Double immunofluorescence staining using human small intestinal tissue showed both Msi-1- and PLA2G2A-expressing IEC's locating at the lowest part of the crypt (Fig. 5, upper series). However, a magnified view showed a clear difference in the distribution of Msi-1- and PLA2G2A-expressing IECs, and not a single cell was found to coexpress both proteins (Fig. 5, lower series). Msi-1 expression appeared to be restricted to a population of IEC's called the basal columnar cells, characterized by columnar morphology with a thin nucleus, which correspond to the cells recently determined to be definite ISCs.[6] In contrast, PLA2G2A expression was restricted to square cells with rich cytoplasm and a round nucleus, confirming its expression in mature Paneth cells. These findings show that although IECs expressing Msi-1 or PLA2G2A both clustered at the lowest part of the crypt, they each formed a distinct population of cells that were either extremely undifferentiated or fully mature, respectively. As this distribution of Msi-1 and PLA2G2A expression in the human intestine is fully consistent with our previous results, the result suggests that Msi-1 might function as a negative regulator of PLA2G2A expression also in vivo, and thereby contribute to maintain the undifferentiated state of ISCs.

Discussion

In the present study, we demonstrated that expression of Msi-1 in LS174T cells not only induced changes in

cell morphology but also suppressed expression of Paneth cell-specific genes such as *PLA2G2A*. Msi-1 appeared to downregulate *PLA2G2A* expression at the mRNA level by a molecular mechanism independent of the Notch- and Wnt- pathways. As we found that mature Paneth cells, residing adjacent to putative ISCs in vivo, completely lacked Msi-1 expression, loss of Msi-1 expression might be a key event during the process of Paneth cell differentiation from ISCs.

Although *Msi-1* has been reported to be a putative marker gene for ISCs, its functional importance has remained largely unknown.[8,9] As one of the common features of stem cells is to remain undifferentiated, suppression of IEC differentiation could be raised as one possible function of Msi-1. Consistent with this, our present study showed a significant decrease of Paneth cell-specific genes upon Msi-1 expression, suggesting that Msi-1 might function as a negative regulator for IEC differentiation. However, no effect was observed upon genes specific to other lineages, such as *MUC-2* (Fig. 2B). These results may further confirm that maintenance of undifferentiated state in ISCs requires involvement of multiple signaling pathways and molecules, including Msi-1.

Concerning the mechanism of Paneth cell differentiation, previous studies have shown that molecular pathways such as Wnt, Notch, and PPAR-β/δ play critical roles in the development of murine Paneth cells.[7,18,21–23] From our present study, however, the molecular mechanism by which Msi-1 suppresses Paneth cell maturation remains unclear, as it appeared to function independently from both the Notch and Wnt pathways. Further analysis of the Msi-1 target gene within IECs may elucidate the molecular function of Msi-1 in Paneth cell maturation.

The importance of the present finding in vivo may be found in the lowest part of the crypt, where two distinct populations of Wnt-activated IECs reside: ISCs and Paneth cells. Although both types of cell express target genes of the canonical Wnt pathway, they are clearly different in terms of differentiation, as one remains extremely undifferentiated while the other is fully mature. This difference may be, at least in part, mediated by expression of Msi-1, through its function of suppressing Paneth cell differentiation. Thus, our results suggest that expression of Msi-1 in Wnt-activated ISCs may be critically required to avoid progression of the differentiation program toward Paneth cells.

In contrast to IEC differentiation, a series of studies have previously described the role of Msi-1 on IEC proliferation. A recent study using gene knockdown of *Msi-1* in colon cancer cells investigated its role in promoting cell proliferation.[24] Also, another study has reported that p21/CIP1/WAF1 is one of the direct targets of Msi-1.[25] Our present study, however, failed to prove increased cell proliferation upon expression of Msi-1 (Fig. 2A). This failure may due to the aberrant activation of the Wnt pathway in LS174T cells, as this pathway is well known to function as a strong promoter of cell proliferation.[26] Although we were able to observe a two- to threefold increase of TOP-Luc activity upon Msi-1 expression, it appeared to have no significant effect on target genes of the canonical Wnt pathway, thus suggesting that the Wnt signaling pathway might be already fully activated, and no additional function could be achieved in LS174T cells.

Another surprising effect of Msi-1 expression was the significant change in cell morphology and colony formation (Fig. 1C). LS174T cells usually grow in an aggregated form and show a piled-up colony of cells. LS174T/Msi-1 cells, however, grew as a flat monolayer and never formed a colony of piled-up cells. These observations suggested that Msi-1 might also regulate arrangement of the cell cytoskeleton, thereby modulating cell–cell contact or cell motility. Such issues remain to be elucidated in future studies.

In conclusion, Msi-1 suppressed expression of Paneth cell-specific genes, including *PLA2G2A*, in IECs. These findings not only suggest that Msi-1 is a negative regulator of Paneth cell differentiation but also provide insight into functional aspects of Msi-1 expression within ISCs.

Acknowledgments. We express our thanks to Dr. Tetsuo Sudo, Dr. Ryoichiro Kageyama, and Dr. Hideyuki Okano for providing plasmids and antibodies, and to Dr. Hisao Fukushima and Dr. Kazutaka Koganei for providing tissue samples. This study was supported in part by Grants-in-Aid for Scientific Research, Scientific Research on Priority Areas, Exploratory Research, and Creative Scientific Research from the Japanese Ministry of Education, Culture, Sports, Science and Technology; the Japanese Ministry of Health, Labour and Welfare; the Japanese Society of Gastroenterology; the Foundation for Advancement of International Science; the Research Fund of Mitsukoshi Health and Welfare Foundation; and the Research Fund of Japan Intractable Diseases Research Foundation.

References

1. Bjerknes M, Cheng H. Gastrointestinal stem cells. II. Intestinal stem cells. Am J Physiol Gastrointest Liver Physiol 2005;289: G381–7.
2. Moore KA, Lemischka IR. Stem cells and their niches. Science 2006;311:1880–5.
3. Scoville DH, Sato T, He XC, Li L. Current view: intestinal stem cells and signaling. Gastroenterology 2008;134:849–64.
4. Nakamura T, Tsuchiya K, Watanabe M. Crosstalk between Wnt and Notch signaling in intestinal epithelial cell fate decision. J Gastroenterol 2007;42:705–10.
5. Crosnier C, Stamataki D, Lewis J. Organizing cell renewal in the intestine: stem cells, signals and combinatorial control. Nat Rev Genet 2006;7:349–59.

6. Barker N, van Es JH, Kuipers J, Kujala P, van den Born M, Cozijnsen M, et al. Identification of stem cells in small intestine and colon by marker gene *Lgr5*. Nature 2007;449:1003–7.
7. van Es JH, Jay P, Gregorieff A, van Gijn ME, Jonkheer S, Hatzis P, et al. Wnt signalling induces maturation of Paneth cells in intestinal crypts. Nat Cell Biol 2005;7:381–6.
8. Potten CS, Booth C, Tudor GL, Booth D, Brady G, Hurley P, et al. Identification of a putative intestinal stem cell and early lineage marker: musashi-1. Differentiation 2003;71:28–41.
9. Kayahara T, Sawada M, Takaishi S, Fukui H, Seno H, Fukuzawa H, et al. Candidate markers for stem and early progenitor cells, Musashi-1 and Hes1, are expressed in crypt base columnar cells of mouse small intestine. FEBS Lett 2003;535:131–5.
10. Imai T, Tokunaga A, Yoshida T, Hashimoto M, Mikoshiba K, Weinmaster G, et al. The neural RNA-binding protein Musashi1 translationally regulates mammalian numb gene expression by interacting with its mRNA. Mol Cell Biol 2001;21:3888–900.
11. Matsumoto T, Okamoto R, Yajima T, Mori T, Okamoto S, Ikeda Y, et al. Increase of bone marrow-derived secretory lineage epithelial cells during regeneration in the human intestine. Gastroenterology 2005;128:1851–67.
12. Okabe M, Imai T, Kurusu M, Hiromi Y, Okano H. Translational repression determines a neuronal potential in Drosophila asymmetric cell division. Nature 2001;411:94–8.
13. Okano H, Imai T, Okabe M. Musashi: a translational regulator of cell fate. J Cell Sci 2002;115:1355–9.
14. Oshima S, Nakamura T, Namiki S, Okada E, Tsuchiya K, Okamoto R, et al. Interferon regulatory factor 1 (IRF-1) and IRF-2 distinctively up-regulate gene expression and production of interleukin-7 in human intestinal epithelial cells. Mol Cell Biol 2004;24:6298–310.
15. Tsuchiya K, Nakamura T, Okamoto R, Kanai T, Watanabe M. Reciprocal targeting of Hath1 and beta-catenin by Wnt glycogen synthase kinase 3beta in human colon cancer. Gastroenterology 2007;132:208–20.
16. Aragaki M, Tsuchiya K, Okamoto R, Yoshioka S, Nakamura T, Sakamoto N, et al. Proteasomal degradation of Atoh1 by aberrant Wnt signaling maintains the undifferentiated state of colon cancer. Biochem Biophys Res Commun 2008;368:923–9.
17. Ayabe T, Ashida T, Kohgo Y, Kono T. The role of Paneth cells and their antimicrobial peptides in innate host defense. Trends Microbiol 2004;12:394–8.
18. Mori-Akiyama Y, van den Born M, van Es JH, Hamilton SR, Adams HP, Zhang J, et al. SOX9 is required for the differentiation of Paneth cells in the intestinal epithelium. Gastroenterology 2007;133:539–46.
19. Pinto D, Gregorieff A, Begthel H, Clevers H. Canonical Wnt signals are essential for homeostasis of the intestinal epithelium. Genes Dev 2003;17:1709–13.
20. Wang XY, Yin Y, Yuan H, Sakamaki T, Okano H, Glazer RI. Musashi1 modulates mammary progenitor cell expansion through proliferin-mediated activation of the Wnt and Notch pathways. Mol Cell Biol 2008;28:3589–99.
21. Yang Q, Bermingham NA, Finegold MJ, Zoghbi HY. Requirement of Math1 for secretory cell lineage commitment in the mouse intestine. Science 2001;294:2155–8.
22. Suzuki K, Fukui H, Kayahara T, Sawada M, Seno H, Hiai H, et al. Hes1-deficient mice show precocious differentiation of Paneth cells in the small intestine. Biochem Biophys Res Commun 2005;328:348–52.
23. Varnat F, Heggeler BB, Grisel P, Boucard N, Corthesy-Theulaz I, Wahli W, et al. PPARbeta/delta regulates paneth cell differentiation via controlling the hedgehog signaling pathway. Gastroenterology 2006;131:538–53.
24. Sureban S, May R, George R, Dieckgraefe B, Mcleod H, Ramalingam S, et al. Knockdown of RNA binding protein musashi-1 (Msi-1) leads to tumor regression in vivo. Gastroenterology 2008;134:1448–58.
25. Battelli C, Nikopoulos GN, Mitchell JG, Verdi JM. The RNA-binding protein Musashi-1 regulates neural development through the translational repression of p21WAF-1. Mol Cell Neurosci 2006;31:85–96.
26. van de Wetering M, Sancho E, Verweij C, de Lau W, Oving I, et al. The beta-catenin/TCF-4 complex imposes a crypt progenitor phenotype on colorectal cancer cells. Cell 2002;111:241–50.